

Studying β -decay rates in stellar interiors – the PANDORA project



Università
degli Studi
di Catania

How can we query nature to determine nuclear
inputs in the cosmos?



Bharat Mishra on behalf of the PANDORA collaboration

12 May 2021
Virtual Event

Dipartimento di Fisica e Astronomia “Ettore Majorana”, Università degli Studi di Catania, Catania, Italy
Istituto Nazionale di Fisica Nucleare – Laboratori Nazionali del Sud, Catania, Italy

WHAT

Quantity of interest

- β -decay rates in stars
- Atomic environment affects $t_{1/2}$
- Stars are plasma, presence of CSD leads to interesting physics



WHY

Motivation

- Astrophysics models require multiple inputs
- Stellar nucleosynthesis above Fe an interplay between decay and n,p-absorption
- Uncertainties remain in σ_{abs} and $t_{1/2}$



HOW

Plasma modelling and γ -tagging

- Connecting ECR plasma properties to decay rates
- Multi-diagnostic and constant monitoring of plasma
- Measurement of β -decay lifetime using secondary γ -rays

5 general types of decays

$$({}^A_Z X_N)^x \rightarrow ({}^A_{Z+1} Y_{N-1})^{x+1} + e^- + \bar{\nu}_e \quad (\text{continuum state } \beta^- \text{ decay})$$

$$({}^A_Z X_N)^x \rightarrow ({}^A_{Z+1} Y_{N-1})^x + e^- + \bar{\nu}_e \quad (\text{bound state } \beta^- \text{ decay})$$

$$({}^A_Z X_N)^x \rightarrow ({}^A_{Z-1} Y_{N+1})^{x-1} + e^- + \nu_e \quad (\text{continuum state } \beta^+ \text{ decay})$$

$$({}^A_Z X_N)^x + e^- \rightarrow ({}^A_{Z-1} Y_{N+1})^x + \nu_e \quad (\text{orbital EC})$$

$$({}^A_Z X_N)^x + e^- \rightarrow ({}^A_{Z-1} Y_{N+1})^{x-1} + \nu_e \quad (\text{free electron EC})$$

Spontaneity determined by Q-value

$$Q_0 = \begin{cases} q_0 & \text{continuum and bound state } \beta^- \text{ decay, orbital EC} \\ q_0 - 2m_e c^2 & \text{continuum state } \beta^+ \text{ decay} \\ q_0 + K_e & \text{free EC} \end{cases}$$

where q_0 is

$$[m({}^A_Z X_N) - m({}^A_{Z+1} Y_{N-1})] c^2 + [E_X^* - E_Y^*] + [B_X - B_Y] - [B_{X_x}^* - B_{Y_{x+1}}^*] + [e_{X_{x,k}}^* - e_{Y_{x+1,k'}}^*]$$

Decay rate

$$\lambda = g^2 \frac{m_e^5 c^4 |M_{if}^L|^2}{2\pi^3 \hbar^7} f_L(Z', Q)$$

M_{if}^L is the nuclear matrix element

$$f_L(Z', Q) = \frac{1}{(m_e c)^3} \int_0^{p_{\max}} p^2 q^2 S^L(p, q) F^\pm(Z', p) dp$$

$$f_L(Z', Q) t_{1/2} = \frac{(\ln 2) 2\pi^3 \hbar^7}{g^2 m_e^5 c^4 |M_{if}^L|^2}$$

General
theory

In stars/plasma

Q-value associated with decay channels
changes

$$Q \approx Q_0 + \sum_{x=X_X}^{Z_X-1} \Delta_x - \sum_{x=X_Y}^{Z_Y-1} \Delta_x$$

Multiple decay modes

$$\lambda = \sum_l \sum_L g^2 \frac{m_e^5 c^4 |M_{if}^{LL}|^2}{2\pi^3 \hbar^7} f_L(Z', Q')$$

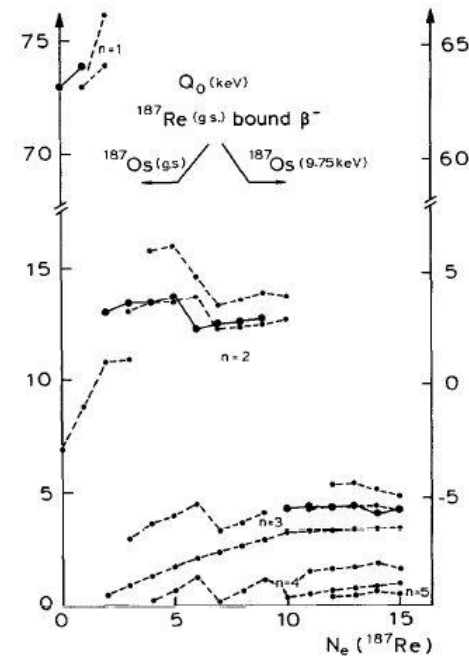
CSD and level population of
plasma ions

EEDF of plasma electrons

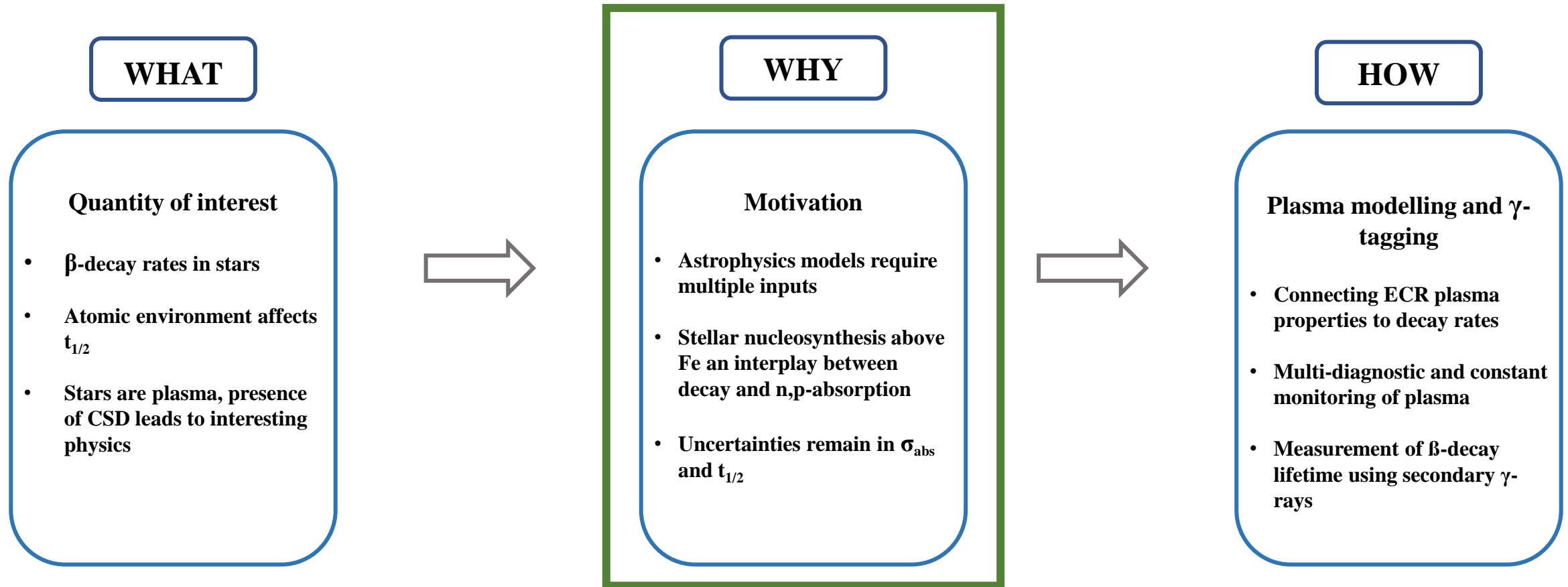
Each decay mode has
associated lepton phase
volume

$$f_{IF(m)}^* = \int_1^{E_{\max}} (E^2 - 1)^{1/2} E q^2 F_0 S_{(m)} f_d dE \quad (\text{continuum decay})$$

$$f_{IF(m)}^* = \sum_y \sigma_y (\pi/2) [g_x \text{ or } f_x]^2 q^2 S_{(m)x} \quad (\text{bound state decays/captures})$$



Q-value of bound state ${}^{187}\text{Re} \rightarrow {}^{187}\text{Os}$
transitions as a function of degree of
ionization [1]



Astrophysical models involve competition between one or more processes

Model usability limited by uncertainty in inputs – $t_{1/2}$, σ_{abs} , $k_B T$, ρ

Solar nucleosynthesis and neutrino flux [2]:

^7Be decay and $^7\text{Be}(p,\gamma)^8\text{B}$ are competing processes, the former produces neutrino flux

Cosmological lithium problem [2]:

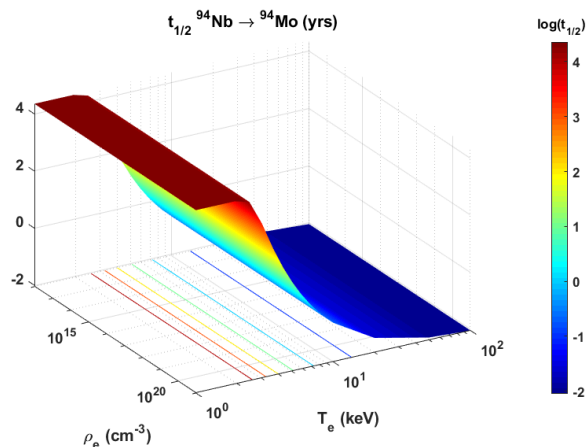
^7Be decay also determines ^7Li abundance, overestimated

S-process branching:

Competition between s-process and decay leads to branching

Cosmochronometers/
Cosmothermometers:

Modification of decay rates can alter use of radionuclides



Modification of half-life as a function of plasma parameters – effect of ion CSD

Nucleosynthesis of ^{134}Ba and ^{136}Ba from ^{134}Cs [3]

Uncertainty in $n \sigma_{\text{abs}}$ and ^{134}Cs $t_{1/2}$

Abundance of ^{94}Nb and ^{94}Mo in presolar SiC grains [3]

Complex model, large uncertainties surrounding s-process in binary AGB star systems

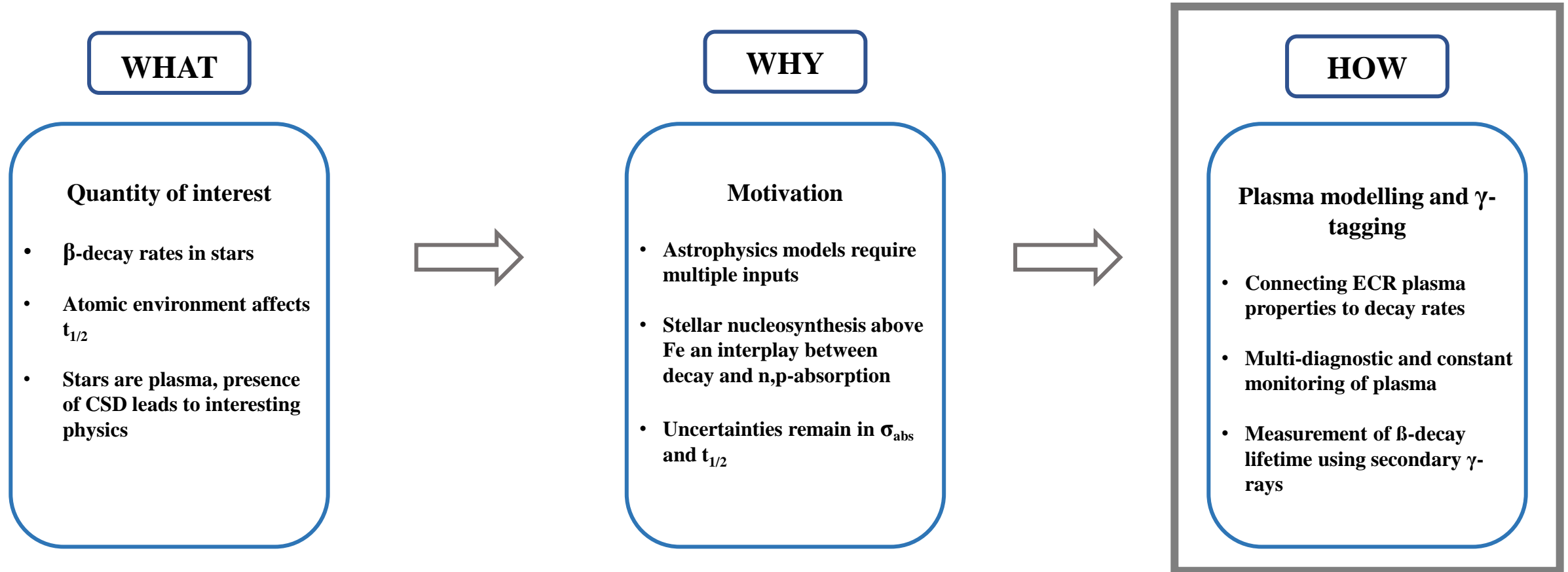
^{176}Lu as cosmochronometer or cosmothermometer [3]

Uncertainties in $t_{1/2}$ as calculated in LTE approach

Temperature effects stronger than density – scalability to astrophysical plasmas

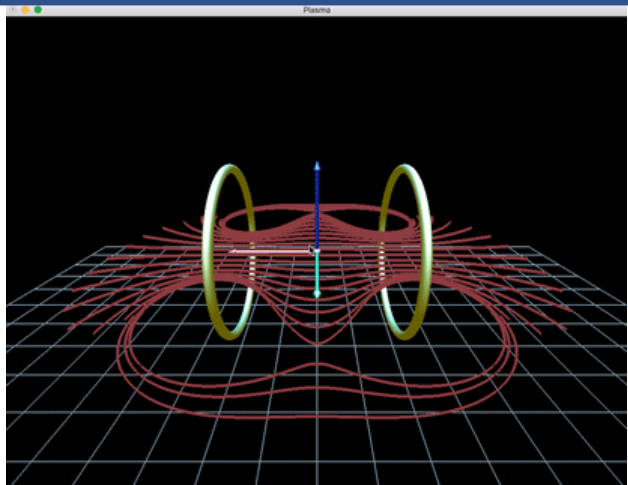
[2] D. Mascalì, A. Musumarra, F. Leone, F.P. Romano, A. Galatà, S. Gammino and C. Massimi, Eur. Phys. J. A 53, 145 (2017).

[3] D. Mascalì *et al*, EPJ Web of Conferences 227, 01013 (2020).



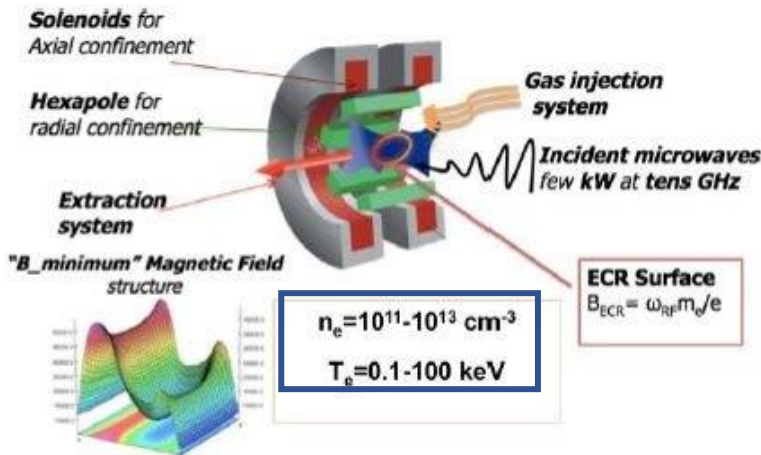
- Stellar interiors are high density and high temperature plasmas
- Experimental validation/correction of theory
- Extrapolation to astrophysical environment

- Magnetic field B applied longitudinally causing electrons to gyrate at frequency $\omega_c = \frac{eB}{m_e}$
- R-wave launched into the plasma at same frequency, leading to resonance heating

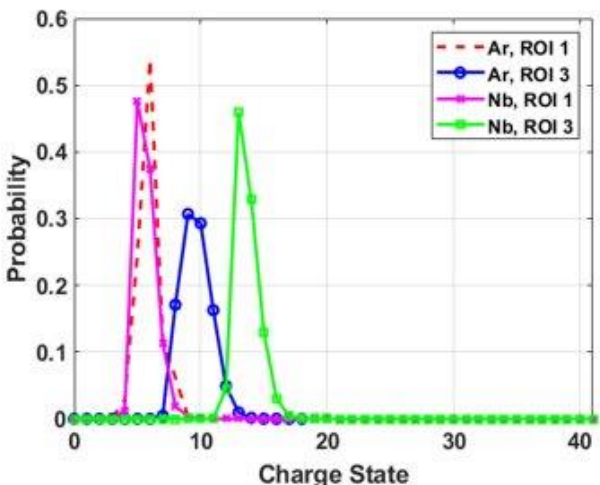


Electron confinement in ECRIS

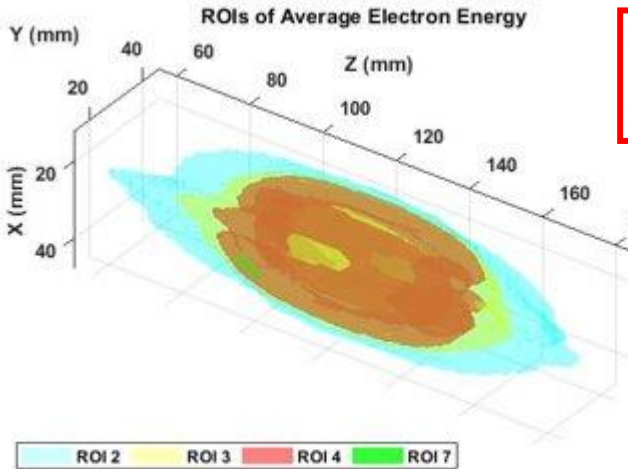
Important properties



Schematic of ECRIS operation and global electron properties [2]



Example of anisotropic ion CSD in ECR plasmas (preliminary model) [5]



Isosurfaces of constant <E> [4]

Model scalable to astrophysical scenarios because T_e dependence measurable (n_e effect negligible!)

ROI	N_e (cm ⁻³)	N_1	kT_1 (eV)	N_2	kT_2 (keV)
1	0	0	—	0	—
2	1.0171E + 15	0.9998	19.0	0.0002	4.2142
3	6.1180E + 14	0.9945	109.9	0.0055	3.0010
4	1.1620E + 15	0.9849	164.7	0.0151	3.1882
5	5.0290E + 14	0.9695	227.2	0.0305	3.2394
6	1.6654E + 14	0.9464	292.6	0.0536	3.3766
7	1.9365E + 13	0.9239	352.0	0.0761	3.5833
8	1.3068E + 12	0.9033	414.6	0.0967	3.7490

[2] D. Mascali, A. Musumarra, F. Leone, F.P. Romano, A. Galatà, S. Gammino and C. Massimi, Eur. Phys. J. A 53, 145 (2017).
[4] B. Mishra *et al*, to be submitted to EPJ D
[5] B. Mishra, A. Pidatella, S. Biri, A. Galatà, A. Mengoni, E. Naselli, R. Rácz, G. Torrisi and D. Mascali, accepted Nuovo Cimento C, 2021

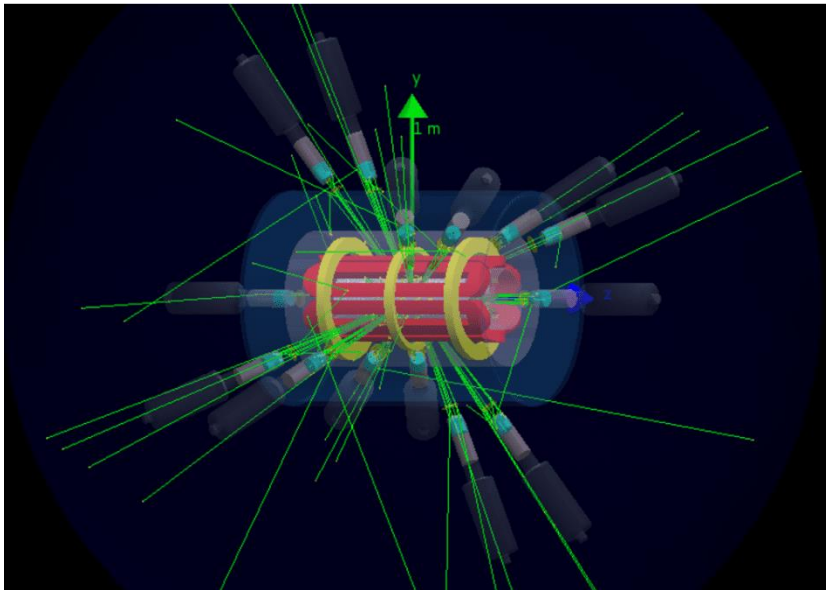
Measurement of $t_{1/2}$: γ -Tagging

8

ECR magnetoplasma can be maintained in MHD equilibrium for days or even weeks

$$\frac{dN}{dt} = \lambda n_i V \longrightarrow N(T_{meas.}) = \lambda n_i V_{plasma} T_{meas.}$$

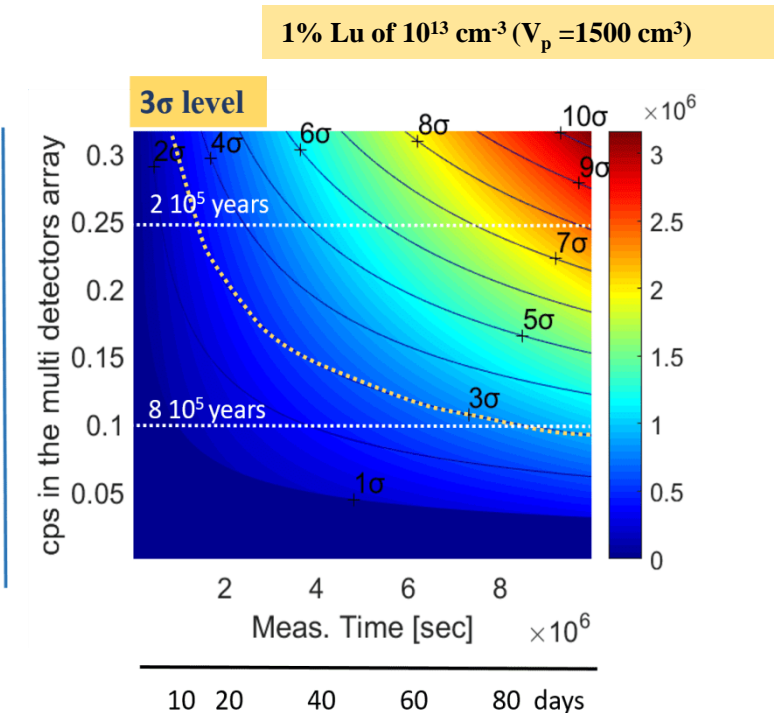
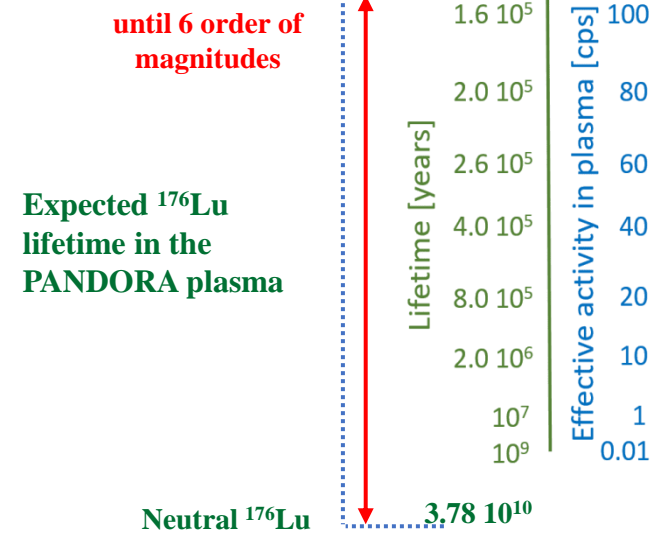
$\lambda n_i V$ is constant
Isotope activity
 $\lambda \equiv \lambda(T, n)$
Density of the isotope in the plasma (const.)
Plasma volume (const.)



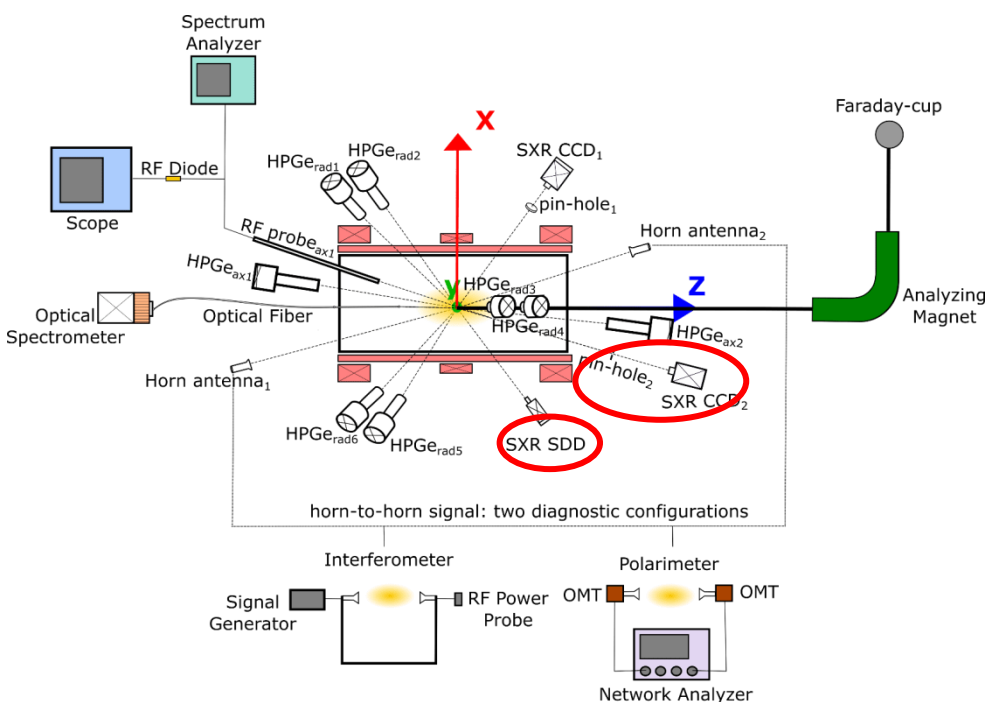
Numerical simulations to determine detection efficiency according to chosen plasma model - 14 HPGe detectors (preliminary model)

Isotope	$T_{1/2}$ [yr]	E_γ [keV]
^{176}Lu	$3.78 \cdot 10^{10}$	202.88 & 306.78
^{134}Cs	2.06	795.86
^{94}Nb	$2.03 \cdot 10^4$	871.09

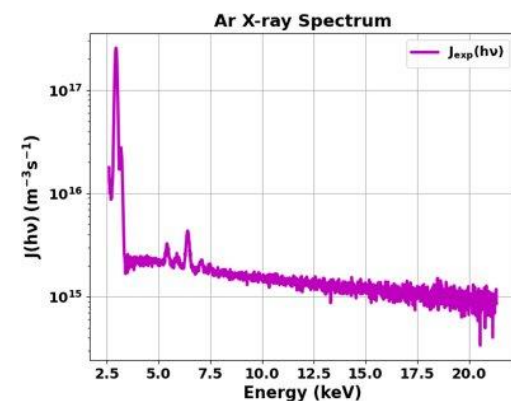
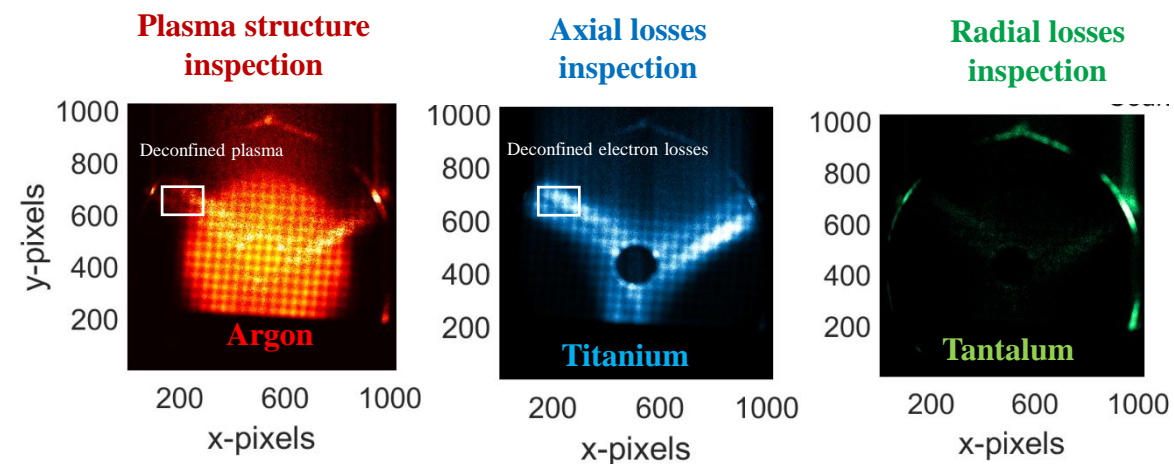
Current models predict measurements lasting from tens of days to a couple of months to obtain a 3σ level of confidence (can be extended to 5σ as well)



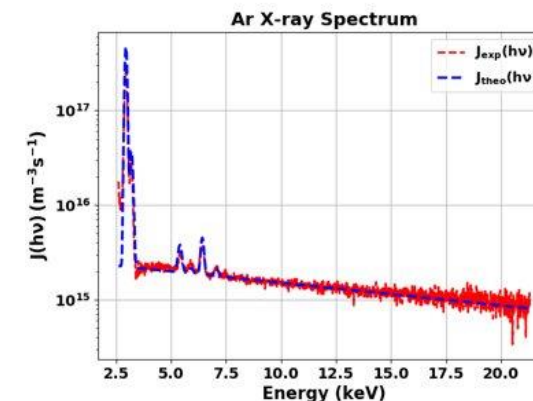
Constant monitoring of plasma density and temperature during acquisition time of paramount importance



Multidiagnostic setup at LNS [6]



$$J_{theo}(h\nu) = J_{theo,brem}(h\nu) + J_{theo,line}(h\nu)$$



Model fit to emissivity density of Ar Plasma [4]

[4] B. Mishra *et al*, to be submitted to EPJ D

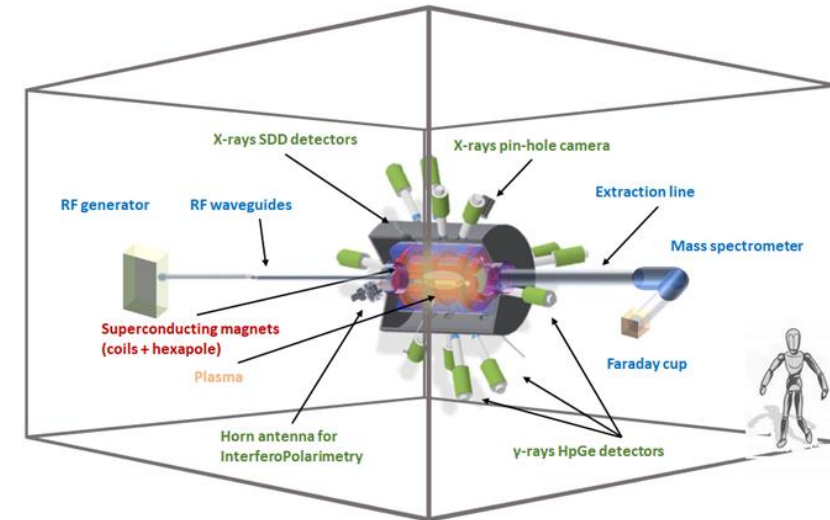
[6] E. Naselli *et al*, Journal of Instrumentation (JINST), 2019

E. Naselli - Invited talk, 3rd European Conference of Plasma Diagnostic, Lisbon (Portugal), 2019

E. Naselli *et al.*, accepted to be published IL NUOVO CIMENTO C, 2021

E. Naselli, Oral - 24th International Workshop on ECR Ion Source (ECRIS), 2020

E. Naselli, Oral - 106th National Congress Italian Physical Society (SIF), 2020



Superconducting
coils for trap

Klystron amplifiers for
microwaves

CCD camera for soft X-
ray detection

HpGe detector array for
 γ -tagging

UNDER PROCUREMENT

IN COLLABORATION WITH GAMMA/GALILEO

β -decay rates one of the most important quantities for astrophysics models

Plasmas in stellar environments influence $t_{1/2}$ – models to predict modification due to CSD exist but need to be verified [1]

Plasmas with relevant properties can be generated through ECR with magnetic confinement

ESTABLISHED

$t_{1/2}$ can be measured in such plasmas, and once theory is verified/improved, can be extrapolated to real astrophysical scenarios – reduce uncertainty

Robust model connecting plasma dynamics with CSD and activity λ of radionuclides

Using MHD-stable plasmas to measure λ using secondary γ -tagging

Multi-diagnostic monitoring to verify system stability for entire duration of experimentation

ONGOING



Sandor Biri
Richard Rácz



David Mascali
Domenico Santonocito
Angelo Pidotella
Eugenia Naselli
Giuseppe Torrisi

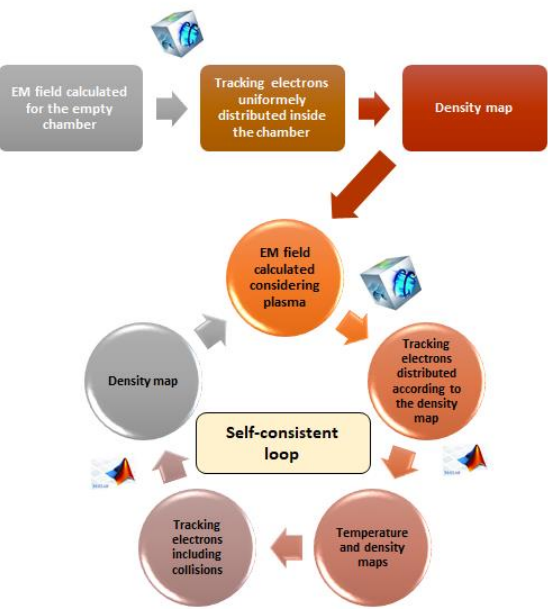


Alessio Galatà

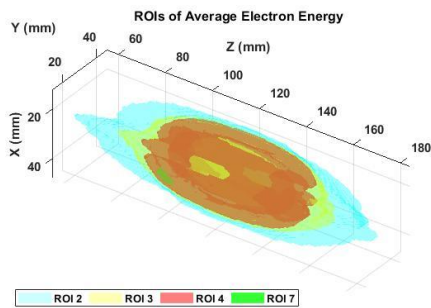


Alberto Mengoni

**THANK YOU
FOR YOUR
ATTENTION!**

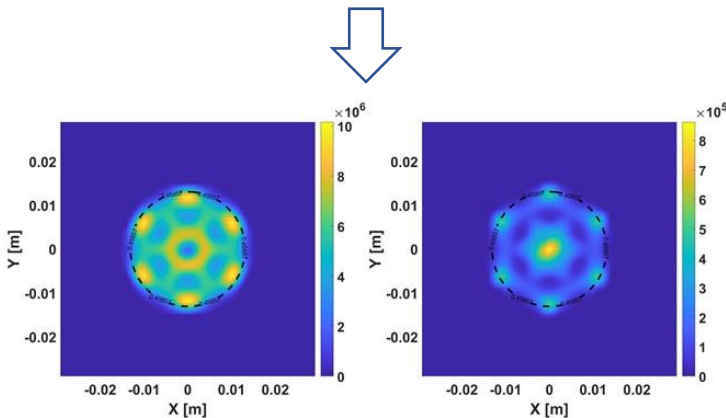


Schematic of COMSOL Multiphysics® + MATLAB® self-consistent numerical modelling for electrons [7]

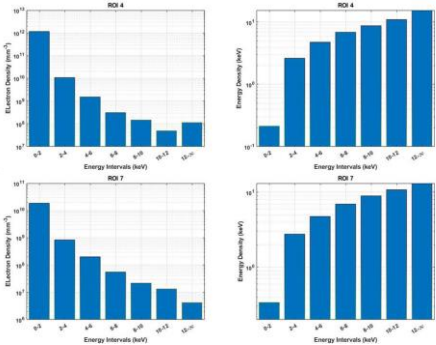


Isosurfaces of constant $\langle E \rangle$

Electron energy and occupation maps intrinsically space-dependent because EM fields involved are anisotropic



XY-projections of occupation maps in [2,4] keV (left) and [6,8] keV (right) [4]



Collective density (left) and energy density (right) in ROI 4 (top) and ROI 7 (bottom)

4 choices of EEDF – mix of Maxwell and Druyvesteyn distribution functions

Ref. case name	Type
EEDF1	Low-E f_M + High-E f_M
EEDF2	Low-E f_M + High-E f_D
EEDF3	Low-E f_M + Medium-E f_M + High-E f_M
EEDF4	Low-E f_M + Medium-E f_D + High-E f_M

$$f_D(E; k_B T_e) = 1.04 \frac{\sqrt{E}}{(\sqrt{k_B T_e})^3} e^{-0.55 E^2 / (k_B T_e)^2}.$$

Each EEDF tested in each ROI – better and more physical analysis

MSE and r^2 calculated for each cell of the ROI, then mean and SD of both quantities evaluated

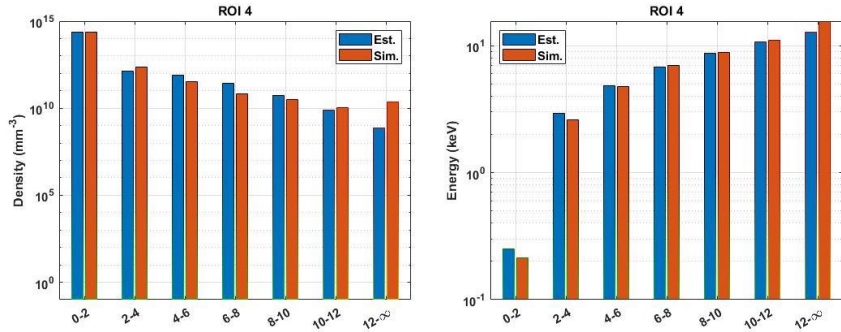
$$\langle MSE \rangle_j = \frac{1}{N(j)} \sum_{k(j)=1}^{N(j)} MSE_{k(j)}, \quad \langle r^2 \rangle_j = \frac{1}{N(j)} \sum_{k(j)=1}^{N(j)} (r^2)_{k(j)},$$
$$\sigma_{(MSE)_j} = \frac{1}{\sqrt{N(j)-1}} \sqrt{\sum_{k(j)=1}^{N(j)} (MSE_{k(j)} - \langle MSE \rangle_j)^2}, \quad \sigma_{(r^2)_j} = \frac{1}{\sqrt{N(j)-1}} \sqrt{\sum_{k(j)=1}^{N(j)} ((r^2)_{k(j)} - \langle r^2 \rangle_j)^2}$$

Mean – average value of the statistic in the ROI

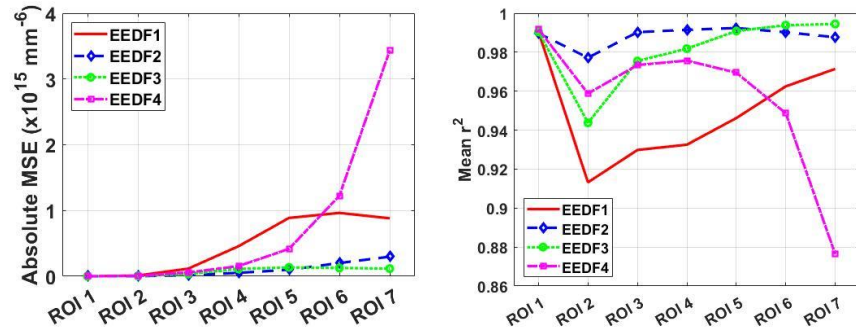
SD – variation of actual value from the mean *within* the ROI

Thus, low mean MSE, high mean r^2 , and low SD for both implies best performance

[4] B. Mishra *et al*, to be submitted to EPJ D
[7] A. Galatà, C. S. Gallo, D. Mascali, and G. Torrissi, e-print arXiv:1912.01988



Simulated density (left) and energy density (right) vs EEDF2 estimate in ROI 3



ROI averaged MSE (left) and r^2 (right) of EEDF2 estimate [4]



New improved simulations of 3D electron maps at higher energy ranges (3-100 keV)

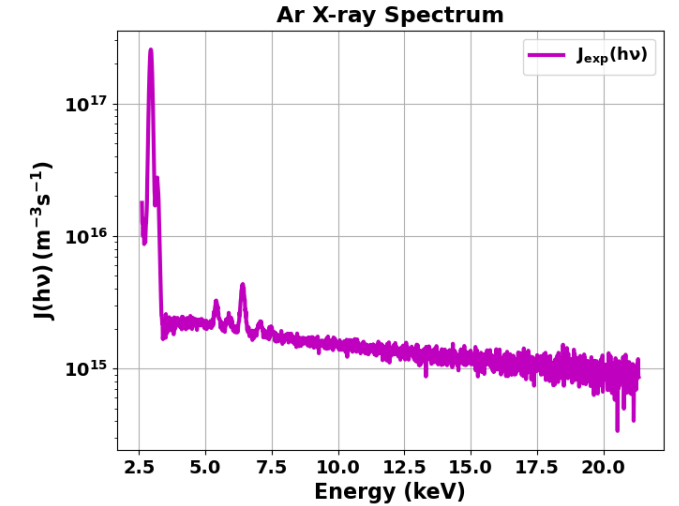


$$J_{theo}(h\nu) = J_{theo,brem}(h\nu) + J_{theo,line}(h\nu)$$

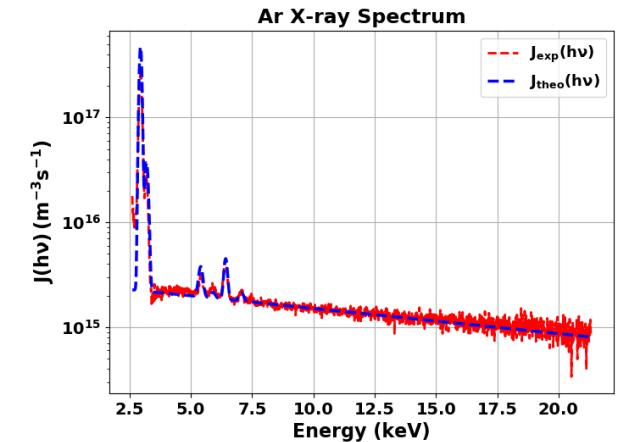
$$J_{theo,K\alpha} = h\nu_{K\alpha} \frac{\rho_e \rho_i \omega_{K\alpha}}{\Delta E} \int_I^{\infty} \sigma_{K,ion} v_e f(E) dE$$

$$J_{theo,K\beta} = h\nu_{K\beta} \frac{\rho_e \rho_i \omega_{K\beta}}{\Delta E} \int_I^{\infty} \sigma_{K,ion} v_e f(E) dE$$

$$J_{theo,brem}(h\nu) = \rho_e \rho_i (Z\hbar)^2 \left(\frac{4\alpha}{\sqrt{6}m_e} \right)^3 \left(\frac{\pi}{kT} \right)^{1/2} e^{(-h\nu/kT)}$$



Emissivity density of Ar Plasma [4]



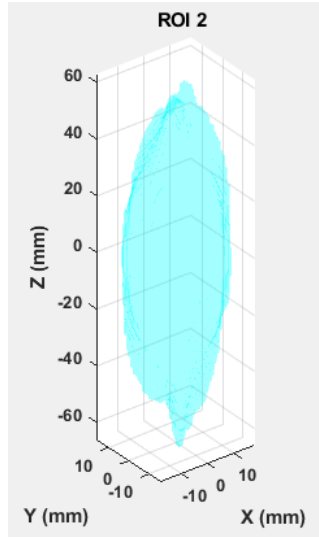
Model fit to emissivity density of Ar Plasma [4]

Each ROI as a single
grand cell

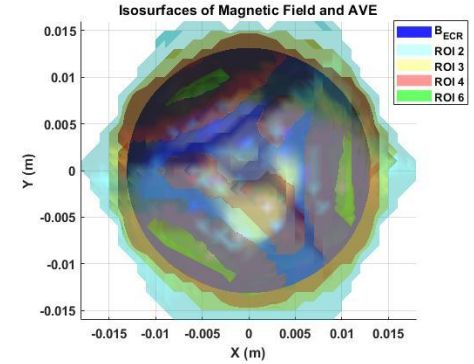
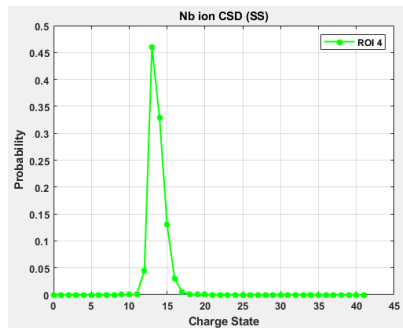
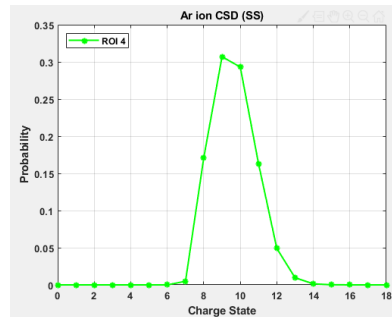
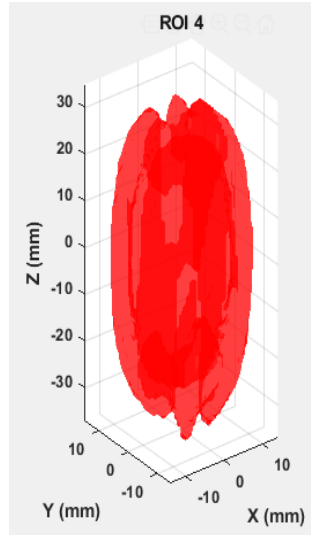
Collective electron
density and EEDF

FLYCHK

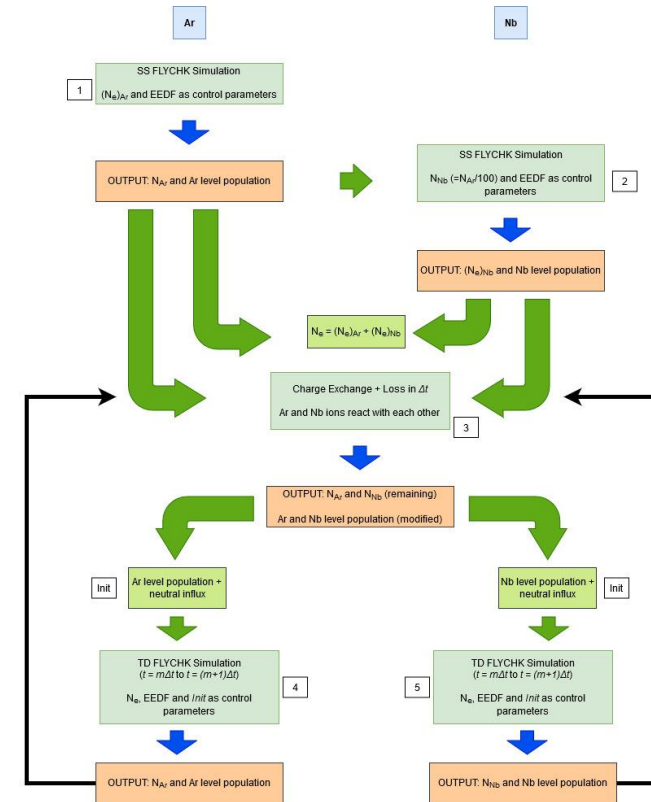
Ion density
Ion CSD
Ion level population



ROI	N_e (cm^{-3})	N_1	kT_1 (eV)	N_2	kT_2 (keV)
1	0	0	—	0	—
2	1.0171E + 15	0.9998	19.0	0.0002	4.2142
3	6.1180E + 14	0.9945	109.9	0.0055	3.0010
4	1.1620E + 15	0.9849	164.7	0.0151	3.1882
5	5.0290E + 14	0.9695	227.2	0.0305	3.2394
6	1.6654E + 14	0.9464	292.6	0.0536	3.3766
7	1.9365E + 13	0.9239	352.0	0.0761	3.5833
8	1.3068E + 12	0.9033	414.6	0.0967	3.7490



Outside ECR: ROI 1, 2, 3 (τ_{halo})
Inside ECR: ROI 4, 5, 6, 7, 8 ($\tau_{plasmoid}$)

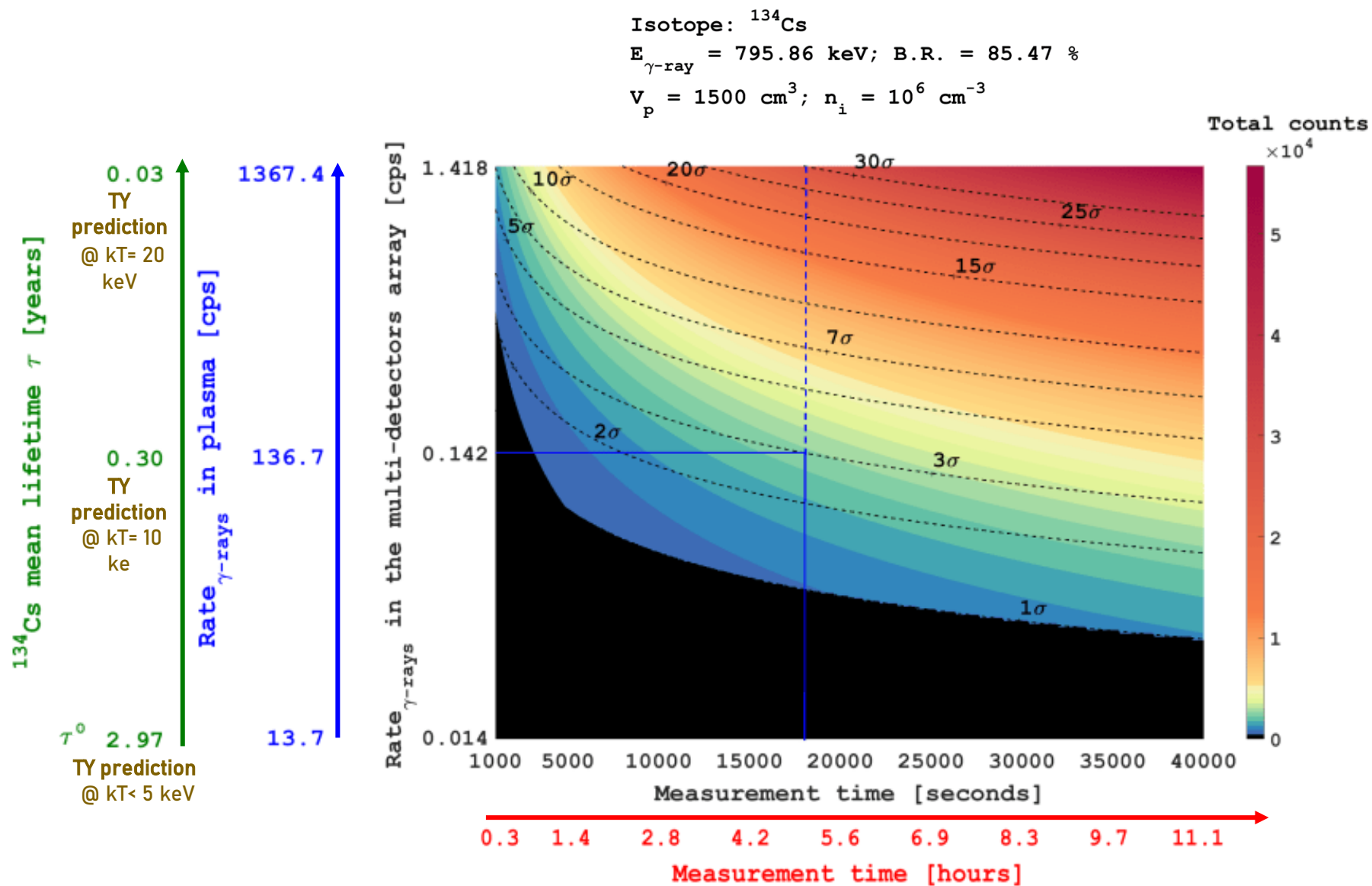


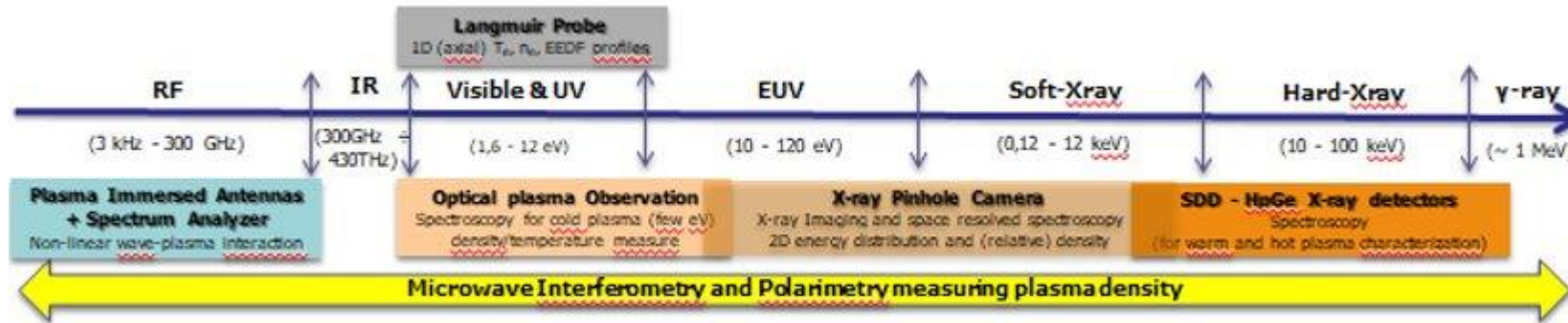
Flow chart showing steps of TD simulation

$$\tau_i^q = 7.1 \times 10^{-20} \left(\frac{l}{2}\right)^2 \ln \Lambda_{ij} \frac{q^2}{T_i^{5/2}} n_e \sum_j \sqrt{A_j} \langle q \rangle_j$$

$$\tau_{ES}^q = \tau_i^q e^{\frac{q \Delta \phi}{k_B T_i}} \frac{1}{\tau_{plasmoid}} = \frac{1}{\tau_i^q} + \frac{1}{\tau_{ES}^q}$$

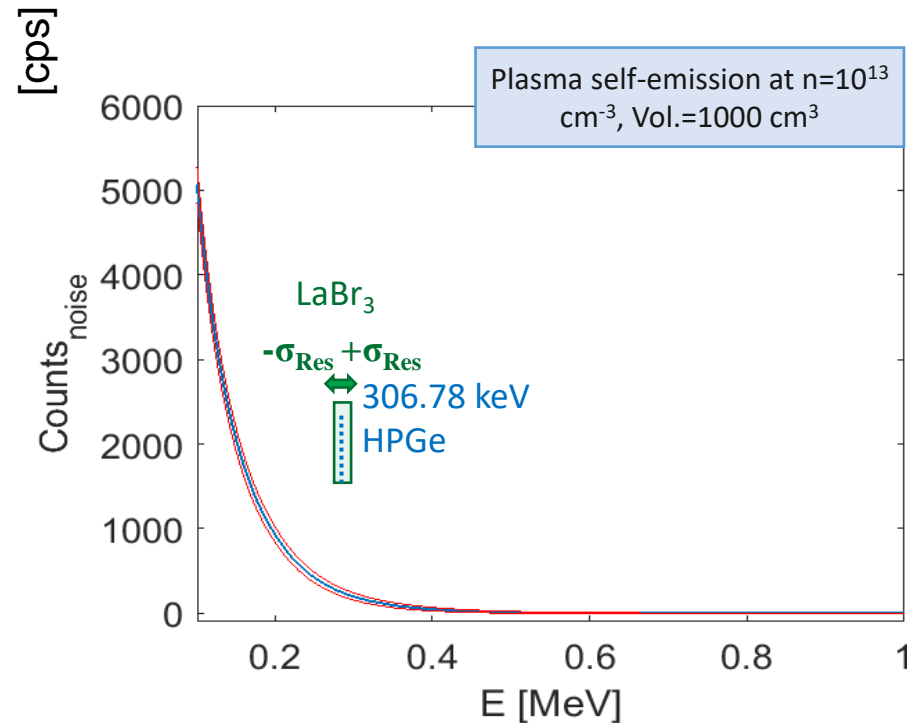
$$\tau_M = R l_h / v T_i \quad \tau_{halo} = \tau_M$$



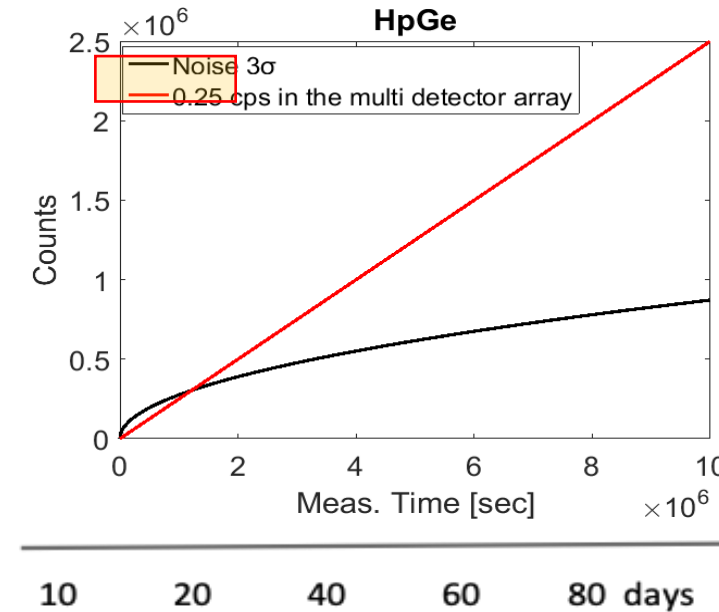


Diagnostic tool	Sensitive Range	Measurement	Resolution & Meas. Error
SDD	1.0 ÷ 30 keV	Volumetric soft X-ray Spectroscopy: warm electrons temperature and density	Res. ~ 120 eV $\epsilon_{n_e} \sim 7\%$, $\epsilon_{T_e} \sim 5\%$
HpGe	30 ÷ 400 keV	Volumetric hard X-ray Spectroscopy: hard electrons temperature and density	Res. ~ 200 eV $\epsilon_{n_e} \sim 7\%$, $\epsilon_{T_e} \sim 5\%$
Visible Light Camera	1.0 ÷ 12 eV	Optical Emission Spectroscopy: cold electrons temperature and density	$\Delta\lambda = 0.04\text{nm}$ R=12500
Microwave Interferometer	K-band 18 ÷ 26.5 GHz	Interferometric measurement: line integrated total density	$\epsilon_{n_e} \sim 50\%$
Microwave Polarimeter	K-band 18 ÷ 26.5 GHz	Faraday-rotation measurement: line integrated total density	$\epsilon_{n_e} \sim 25\%$
X-ray pin-hole camera	2 ÷ 15 keV	2D Space-resolved spectroscopy soft X-ray Imaging and plasma structure	Energy Res. ~ 0.326 keV Spatial Res. ~ 0.56 mm
Multi-pins RF probe + Spectrum Analyzer (SA)	10 ÷ 26.5 GHz (probe)	Frequency-resolved Spectroscopy plasma emitted EM wave in GHz range	SA Resolution bandwidth: RBW = 3 MHz
Multi-pins RF probe + Scope + HpGe	10 ÷ 26.5 GHz (probe)	Time-resolved X-ray Spectroscopy	80 Gs/s (scope) time scales below ns

The noise (consisting, especially, in the plasma self emission) affects the detection of the signal



The noise spectrum was used to evaluate the time needed to have a significant 3 level signal



The intersection from the two lines shows the point where the signal over comes the 3 noise level, and the correspondent abscissa is the measurement time needed to have a 3 level of confidence

Trend of the **signal counts** (in red) compared to the **3 times the noise** (in black)

$$\text{Noise}_{3\sigma} = 3 \sqrt{\text{Noise}_{cps} \cdot T_{meas}}$$

$$N(T_{meas}) = \lambda n_i V_{plasma} T_{meas}$$